Kufa Journal of Engineering
Vol. 16, No. 4, October 2025, P.P. 67-86
Article history: Received 18 September 2024, last revised 23 November 2024, accepted 23 November 2024

AN ENHANCED ALGORITHM TO IMPROVE THE ACCURACY OF LIE DETECTION SYSTEM BASED ON EEG SIGNAL

Ayia A. S. A. Jabar

Assisstant Lecturer, Al-Iraqia University, Baghdad, Iraq,
Email: ayia.abd.abduljabar@aliraqia.edu.iq

https://doi.org/10.30572/2018/KJE/160404

ABSTRACT

In recent years, lie detection has been a prominent focus for many researchers due to its significant influence on criminology and society. A key challenge in numerous investigations has been the system's accuracy, which is heavily reliant on the type of algorithm employed in the classification process. Another critical factor affecting accuracy is the signal-to-noise ratio (SNR). In this paper, we explore a deep learning framework within the lie detection test paradigm. During the signal acquisition phase, EEG signals were recorded using the Natus device. Independent component analysis (ICA) was subsequently applied to remove noise during signal processing. Additionally, regression baseline correction was used to adjust the baseline, followed by averaging to generate event-related potentials (ERP), which resulted in a 23.2% improvement in SNR. Several algorithms were also employed, including support vector machines (SVM), deep belief networks (DBN), and linear discriminant analysis (LDA). Our proposed approach achieved an accuracy of 86% when using the same dataset from previous research, while new data collection from several participants yielded an accuracy of up to 78%.

KEYWORDS

Lie detection, Electroencephalogram, Event-related potential, independent component analysis.

1. INTRODUCTION

For a long time, polygraphs have been used to detect scams by criminals. The principle of this device is based on the physiological changes that occur in the human body while lying or hiding information, such as a rapid heartbeat, high temperature, or weak tone of voice (Lin et al., 2018). This device continued to produce results, but they were inaccurate because these physiological changes could be controlled by using some medications or training (Rad et al., 2023). Therefore, there was an urgent need to use other changes that occur in the body during lying but are difficult to control, such as electroencephalography (EEG) (Gao et al., 2022). EEG is a test in which the electrical activity of brain cells Due to its rich information on human activity, is recorded by placing several sensors on the outer cortex of the head, where each sensor calculates the electrical activity of a specific area of the brain (Obais and Hasan, 2020). A variety of brain-related diseases can be diagnosed and monitored with the use of an EEG. Another important use of brain electrical signals is lying detection, which is done by extracting event-related potential (ERP) signals and then observing the P300, which is used 300 milliseconds (ms) after the stimulation process (Supriya et al., 2023). Therefore, using time resolution, ERPs offer a direct estimate of brain activity that is essential for isolating the neurocognitive processes that happen quickly after a trigger, reaction, or many other events (Kappenman et al., 2021).

Processing the signal is one of the important steps to know the more accurate ERP, as the effect of noise changes the true state of the signal associated with a certain disease or to detect lies. There are many operations on the signal that can be used, the most famous of which are filtering, ICA, and Principal component Analysis (PCA) (Yue, Plested and Gedeon, 2020;Kokate, Pancholi and Joshi, 2021;Gu et al., 2023). The advantage of PCA lies in its ability to reduce the feature space dimension by taking into account the variance of the input data (Ali and Hameed, 2020).

Feature extraction is employed to discern intricate brain wave patterns, wherein a valuable signal is isolated using several parameters that are subsequently utilized for classification. In (Pooja, Pahuja and Veer, 2022), the involved ERPs P300 have utilized an array of features in the time-domain, frequency-domain, and wavelet domain to extract information. This approach aims to develop the system's performance and precision. The subsequent phase involves data classification, employed to ascertain the presence or absence of the provided information on the subject. The predominant approach in this genre of research is the utilization of classification algorithms. These algorithms categorize the resultant data into distinct classification classes, and the efficacy of the classifiers is subsequently evaluated. The classification algorithms most employed are support vector machines (Bablani et al., 2021), multi-layer feed-forward neural networks (Bablani et al., 2020), extreme learning machines (ELM) (Zhou, Zhang and Jiang, 2021), and deep belief networks (Chao and Liu, 2020). Cross-validation is a statistical method used in machine learning to evaluate a model's performance on unseen data. It involves splitting the dataset into multiple subsets to test the model's generalizability. The goal is to ensure the model isn't overfitting or underfitting and performs well across different parts of the data.

The primary objective of this paper is to develop a lie detection method based on EEG signals that cannot be influenced by the individual through training or medication, in order to achieve the highest possible accuracy. This is accomplished by removing noise from the signal using modern signal processing techniques and applying advanced machine learning algorithms. This article is structured into six sections. Section 2 presents a summary of previous studies. The methodology and results are discussed and provided in Sections 3 and 4, while Section 5 covers the experimental protocol. The concluding remarks of the article are given in Section 6.

2. LITERATURE SURVEY

Referring to (Baghel et al., 2020) Convolutional neural networks (CNNs) are used in this study's deep learning methodology to extract the truth from EEG data. The proposed model was trained using EEG data in 14 channels. When this study and another work were compared, the CNN algorithm improved the classification accuracy from 82% to 84%. The gap in this research lies in the classification of the image in a different position, in addition to the interference of electrode signals leading to inaccurate signal processing and consequently inaccurate classification results.

Referring to (Xiong, Gu and Gao, 2020) The phase synchronization (PS) method was applied in this paper. He attempted to get further insight into the basic mechanism of deception by analyzing the spread of electrodes based on the outcomes of the phase synchronization (PS) patterns across 12 EEG channels. Phase locking value (PLV) from PS was used as a statistical tool for regression or classification for minimum stimuli in the lie detection test. In particular, the classification approach yields findings with a high accuracy of up to 88%. Methodological challenges regarding quantifying functional connectivity through PS analysis have been extensively explored, yet some remain unresolved. For instance, the optimal duration of EEG signal segments for estimating the PS index hasn't been definitively determined. Additionally, identifying the most appropriate methods for inferring the significance level of the estimated PS index remains an ongoing concern.

Referring to (Rahmani et al., 2024) the study presents an automatic model for detecting truth from lies using EEG signals. An EEG database of 20 study participants was created to accomplish this goal. This study also used a six-layer graph convolutional network and type 2 fuzzy (TF-2) sets for feature selection/extraction and automatic classification. The classification results show that the proposed deep model effectively distinguishes between truths and lies. As a result, the classification accuracy nearly 90%.

Referring to (Gao et al., 2022) the study aimed to explore the brain's functional connectivity (FC) patterns during lie detection activities, shedding light on the underlying brain activities linked to deception. Electroencephalogram (EEG) data were collected using 32 electrodes, with a focus on analyzing EEG phase synchrony among different brain regions. To mitigate the risk of false synchronization from volume conduction, the researchers introduced Few-Trials-Based Relative Phase Synchrony (FTRPS) as a measurement. The features extracted for analysis encompassed FTRPS values derived from the FC networks. The classification process employed the SVM technique to distinguish between instances of deception and truthfulness. The gap in this study lies in the limited number of trials used in FTRPS, leading to difficulty in applying the work to diverse cases differing from the proposed one.

Referring to (Wei et al., 2023) this paper explores how brain network's function while people are lying, revealing patterns of information exchange within neural oscillations. Using EEG data collected from forty participants who were either lying or speaking the truth, weight-directed functional brain networks were constructed. With an amazing accuracy rate of 85.93%, the analysis throughout all frequency bands correctly identified dishonesty and innocence.

As noticed from the Table 1, there are a few disadvantages or drawbacks related to detection falsehoods, this research clearly proposes a framework for improving the accuracy of detection falsehoods using EEG signals. The signals are recorded with an EEG device, and a signal processing module applies various methods to obtain P300-ERP signals. Subsequently, feature extraction is performed, and machine learning algorithms are suggested for classification.

Table 1. Methodology and accuracy of literature survey

Ref.	Signal Acquisition	Signal Processing	Feature extraction and classification	Accuracy
(Baghel et al., 2020)	14 channel device	-	CNN	84%
(Xiong, Gu and Gao, 2020)	12 channel device	PS patterns	PLV	88%
(Rahmani et al., 2024)	16 channel device	Bandpass filter	GCN with TF-2	90%
(Gao et al., 2022)	32 electrode device	FTRPS	SVM	93%
(Wei et al., 2023)	12 channel device	-	WDFBN	85.93%

3. METHODS

This section outlines the suggested lie detection system, illustrated in Fig. 1, and elucidates the operational steps involved in its implementation. The process encompasses the utilization of a signal acquisition device and signal processing employing various techniques such as ICA and regression-based baseline correction. These techniques aid in transforming data epochs into ERPs with a precise baseline. The subsequent stages involve feature extraction, responsible for extracting features from ERP signals, and classification utilizing the Support Vector Machine algorithm. This algorithm serves to determine whether an individual is being truthful or deceptive based on the classified ERP signals. This proposed system has been implemented in the following steps:

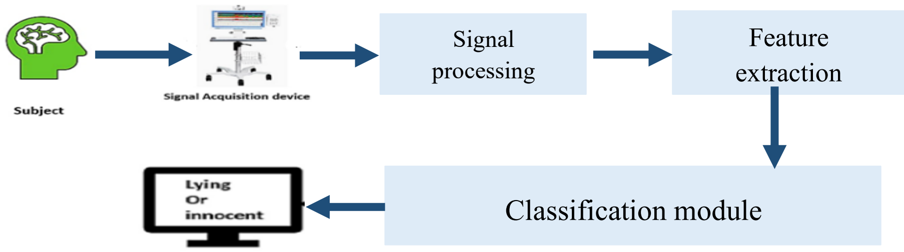

Fig. 1. The proposed lie detector system.

3.1. Signal Acquisition

Collect data from the EEG device, the objective of this process is to obtain data that can be processed by a computer and read in Python language. The data is extracted in CSV format.

3.2. Signal Processing

The goal of this step is to process the noise present in the signal, which significantly affects the classification accuracy of the signals. This is achieved by obtaining a high signal-to-noise ratio. Commencing the practical procedures in this phase involves the utilization of the Python programming language, specifically version 2.9. Essential libraries like NumPy, Pandas, Matplotlib, and SciPy are employed for various functionalities. Moreover, the primary MNE-python library plays a pivotal role in reading and processing EEG signals.

3.3. Feature Extraction

The feature extraction aims to differentiate the characteristics of the event-related potential signal between instances of deceit and honesty. The choice of feature extraction approaches was made to evaluate their impact on the decision-making process regarding the truthfulness of the individual.

3.4. Classifications

In this step, the signal is classified to determine whether it belongs to a truthful or deceptive individual. This is achieved by employing multiple machines learning algorithms and selecting the algorithm that provides the highest accuracy.

4. PRACTICAL METHODOLOGY

In this section, operational details of the methods used in each step of the workflow are elucidated. The Neurotech device is utilized for signal extraction, followed by signal processing using ICA and Regression baseline correction. Features are then extracted from the signal in both the time domain and time-frequency domain. Subsequently, classification is performed, and the algorithm yields the highest accuracy, such as (DBN), (SVM), and (LDA).

4.1. Signal Acquisition

The Nicolet v32 Modular Neurodiagnostic System was used which has a feature of 32 channels and sample rate of up to 2KHz.

4.2. Signal Processing

As depicted in the flowchart in Fig. 2, the EEG data acquired from the device is read in CSV format, and subsequently, diverse signal processing techniques are applied. One of these techniques called regression-based baseline correction are used to EEG signal aiming to achieve the highest SNR. A greater SNR is typically preferred in signal processing applications since it denotes a better and more dependable signal. In the context of signal in EEG, the SNR can be calculated by the following equation:

$$SNR_{db} = 10log_{10}(\frac{variance_{signal}}{variance_{noise}}) \quad (1)$$

The improvement in SNR values can be achieved through the applied of noise removal theories. To assess the enhancement in the signal, the change in SNR can be calculated before and after employing these theories as illustrated in the following equation:

$$\Delta SNR_{db} = 10log_{10}\left(\frac{variance_{signal}}{variance_{noise}}\right)_{after\ denoising} - 10log_{10}\left(\frac{variance_{signal}}{variance_{noise}}\right)_{before\ denoising} \quad (2)$$

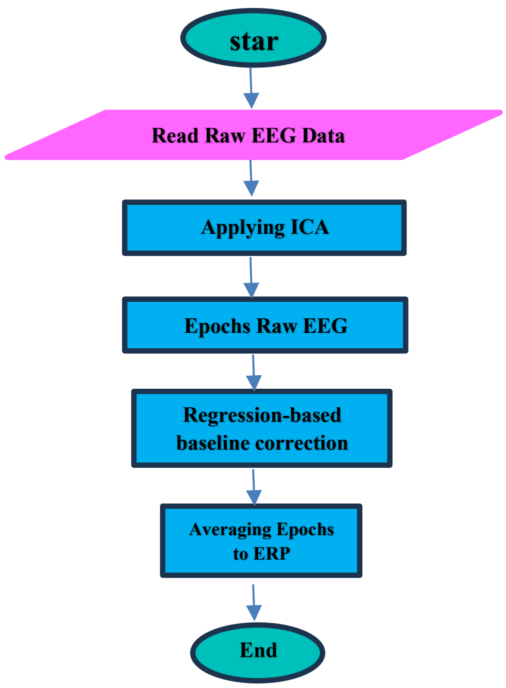

Fig. 2. Signal processing module flowchart.

4.2.1. Read Data

The first step in the flowchart in Fig. 3 is to read the CSV data that was taken from the EEG device. This is done by using the Pandas Python module, which controls the reading process. Electrodes placed on the scalp were used to extract 14 channels. These channels include vertical electrooculography (VEOG), horizontal electrooculography (HEOG), FP1, FP2, F3, FZ, F4, C3, CZ, C4, P3, PZ, P4, OZ, and P3. The channel names and their placements according to the 10–20 montage are included in the data, as shown in Fig. 3.

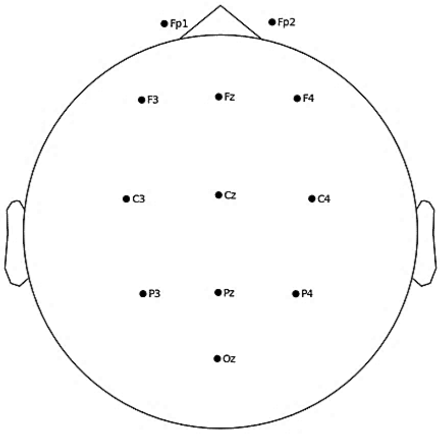

Fig. 3. Location of the electrodes of raw data.

4.2.2. Independent Component Analysis (ICA)

Using a set of recordings where the ratios of the source signals' mixtures are unknown, ICA is used to accurately predict information from the source signals. This method is used in this work to reduce the noise influence from the VEOG and HEOG channels, which is caused by the subject's eye movements. As seen in Fig. 4, the electrodes are positioned above, below, right, and left of the eyes.

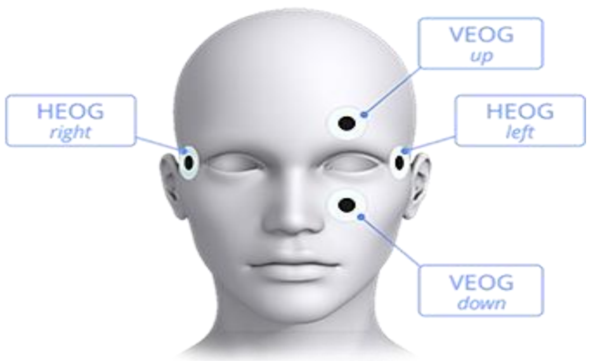

Fig. 4. Location of HEOG and VEOG electrodes. (Obais and Hasan, 2020)

The first step of ICA process is estimated independent components (ICs) by using Singular Value Decomposition (SVD) theory and reconstructed raw data in the second-step by omit designed components from the signal using the unmixing matrix, alter the data, zero out all excluded components, and reverse transform the data.

4.2.3. Epoch EEG Signals

Using this method, the raw EEG data is divided into epochs according to the kind of occurrence (probe, irrelevant, and target). As a result, the raw data matrix will get an additional dimension, changing its original format from (channel * time) to (channel * time * event). The division of raw data into several epochs is displayed in Fig. 5. Eq. (3) (Kokate, Pancholi and Joshi, 2021) illustrates the raw data epochs procedure (Obais and Hasan, 2020).

$$X_{ij}(t) = x_{ij}(t - t_{ij}) \qquad \text{for } t = 0, 1, 2, \ldots, t_{max} - 1 \qquad (3)$$

Where $X_{ij}(t)$ is the EEG signal for the i_{th} trial and j_{th} electrode, $x(t)$ is the raw EEG signal, and t is the time of i_{th} event for the j_{th} electrode and $t_{max}$is symbolizes the end of the interval's maximum time point.

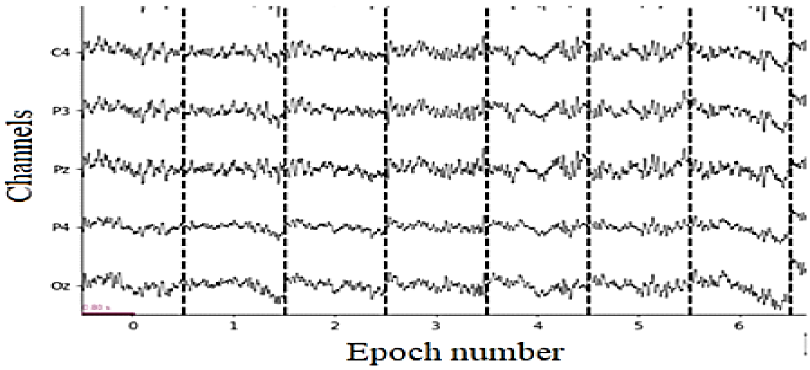

Fig. 5. Epochs raw data.

4.2.4. Averaging Epochs using Regression-Based Baseline Correction

Based On generating the event-related potential, this work computes the average of the epoch group, as demonstrated in Fig. 6. This process may introduce baseline drift due to the noise present in each epoch, necessitating baseline correction. Initially, for illustrative purposes, traditional baseline correction is applied to grasp the distinction between traditional and regression-based baseline correction. In practical terms, the first step involves defining the baseline period, which serves as a reference for comparing the rest of the signal in each epoch. In this study, this period corresponds to the pre-stimulus interval, as the brain is in a stable state during this time. Eq. (4) outlines this period (Obais and Hasan, 2020).

$$Baseline - \text{interval} = t_{\max} - t_{\min} \qquad (4)$$

$\boldsymbol{t_{max}}$: symbolizes the end of the interval's maximum time point.

$\boldsymbol{t_{min}}$: signifies the lowest point in time at which the interval begins.

In the traditional baseline approach, the following adjustment method is applied individually to each epoch

1) Determine the baseline period mean signal
2) Take this mean and subtract it from the total epochs

Fig. 7 (a), and (b) illustrate the ERP with traditional baseline correction, and regression baseline correction respectively.

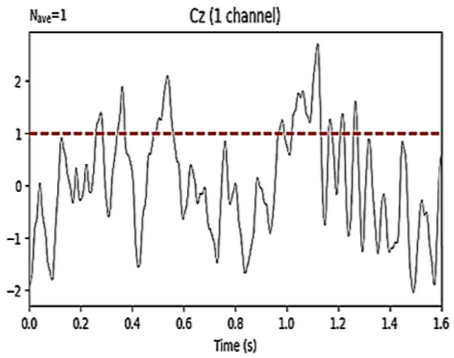

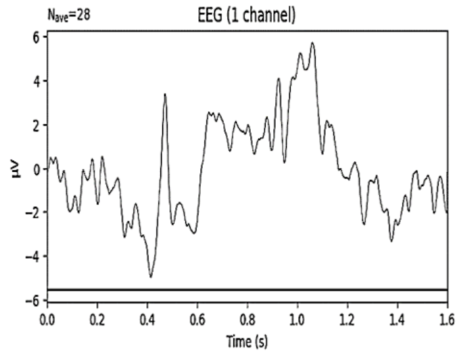

(a) **(b)**

Fig.6. (a) Average signal (ERP) with traditional baseline correction;
(b) average signal (ERP) with regression baseline correction.

4.3. Feature Extraction

the goal of feature-extraction in this research is to identify the differences-in the properties of the ERP-signal between lying and-truthful states. therefore, the selection-of feature extraction was based on decision-making regarding whether the person-was lying or not. In this study, Multiple features-were tested, but those found to have-negligible impact on decision-accuracy were omitted from the model to ensure its effectiveness and-relevance. Fig. 7 depicts the selected features and assesses the influence of each on decision accuracy.

4.3.1. Time-Domain Features

The pre-processed data was structured as a matrix, where each row represented an individual's ERP signal and the columns indicated the amplitude at intervals of 0.002 seconds within a time window of 0 to 1.6 seconds. For this study, the focus is on the time interval between 1.1 and 1.3 seconds, as changes in the signal occur following the stimulus, which was triggered at 1.1 seconds. Therefore, the matrix segment corresponding to the 1.1 to 1.3-second range was extracted, and the following features were calculated:

- maximum amplitude: $A_{max} = max_n|x(n)|$, where A_{max} is the maximum amplitude, $x(n)$ is the sampled signal, n represents discrete time indices.

- minimum amplitude: $A_{min} = min_n|x(n)|$,

- standard deviation: $\sigma = \sqrt{\frac{1}{N}\sum_{n=1}^{N}[x[n] - \mu]^2}$ where µ is the mean of signal and N is the total number of samples.

- positive area amplitude: $A_{pos} = \sum_n \max(0, x[n])$

4.3.2. Time-Frequency Domain Features

First, use Eq. (5) (Wei et al., 2023) to find the time-frequency representation of the data using Morlet wavelets (which frequently used for the analysis of time-frequency in non-stationary time series data, such as brain-recorded neuroelectric signals). Based on Morlet wavelet, the time-frequency resolution can be adapted to different signals of interest.

$$\psi(t) = Ae^{\left(-\frac{t^2}{2\sigma^2}\right)}.\cos(2\pi f_0 t) \tag{5}$$

where A is a normalizing constant used to guarantee that the wavelet has unit energy, σ is the Gaussian envelope's standard deviation, and f_0 is the wavelet's central frequency. Next, compute the average value throughout a time-frequency diagram.

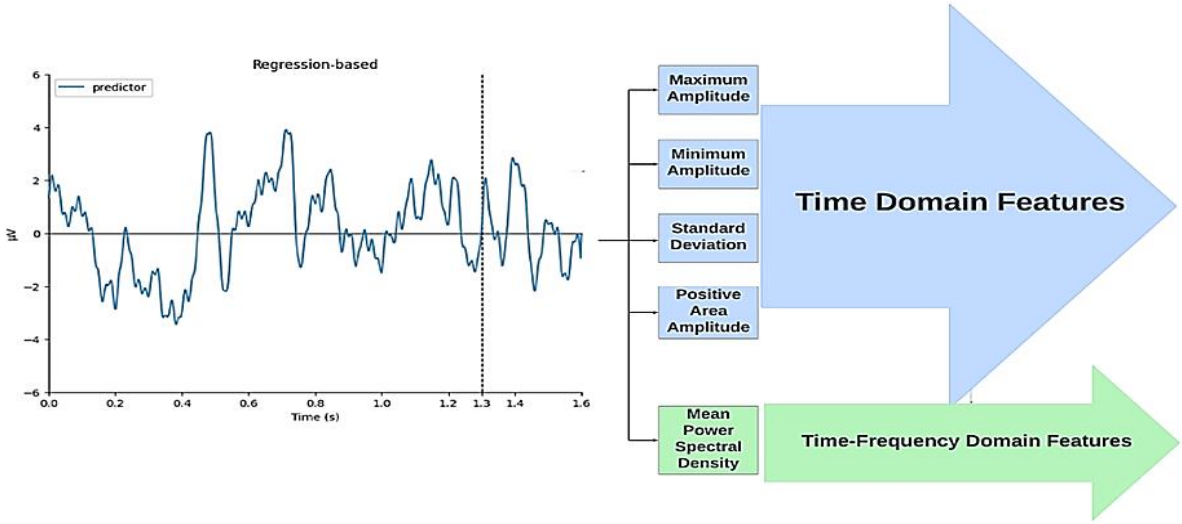

Fig. 7. Features extraction from ERP signal.

4.4. Classification

Following the extraction of features from the ERP signal across multiple samples, the resulting row matrix represents the number of samples, with columns denoting the number of features. The construction of the DBN, SVM, and LDA algorithms was implemented through the MNE-python library, following the steps outlined below:

4.4.1. Data Representation

Each data point is represented as a feature vector within a high-dimensional space. Fig. 8 visualizes the data distribution by selecting only two features to enhance clarity in illustrating the distribution and discerning the chosen function.

4.4.2. Radial Basis Function (RBF) Kernel Function

Kernels are essential in transforming data into higher-dimensional spaces, allowing algorithms to capture complex patterns and relationships. Among the various kernel functions, the Radial

Basis Function (RBF) kernel is particularly notable for its versatility and effectiveness.

Also known as the Gaussian kernel, is defined as (Bablani et al., 2021):

$$K(x_i, x_j) = e^{\left(-\frac{\|x_i - x_j\|^2}{2\sigma^2}\right)} \tag{6}$$

Where σ is a parameter that controls the Gaussian distribution's width.

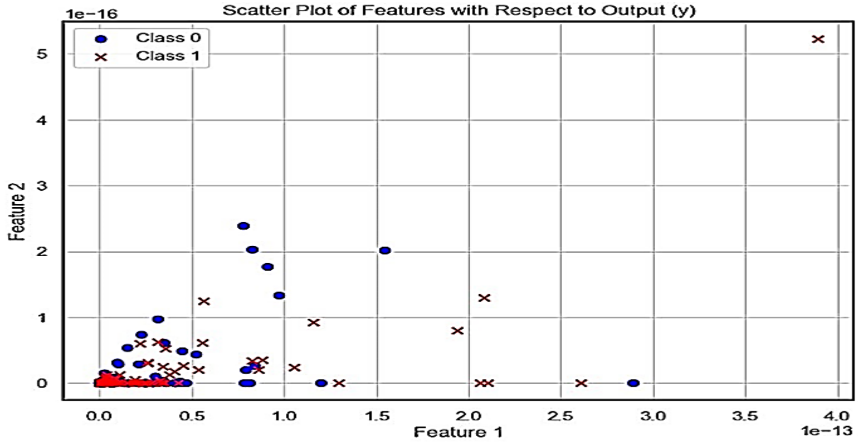

Fig. 8. Two feature distributions concerning output.

4.4.3. SVM Decision Function

The support vector machine is a cutting-edge classification algorithm with a strong theoretical basis in statistical learning theory (Vapnik, 1995). Rather than focusing on minimizing misclassification errors on the training set, SVM employs structural risk minimization to define the decision function, helping to prevent overfitting.

The expression for the decision function in SVM using a Radial Basis Function (RBF) kernel is (Bablani et al., 2021):

$$f(x) = \sum_{i=1}^{N} \alpha y_i K(x_i, x_j) + b \tag{7}$$

Where α is constant; in this case, experimentation is used to discover this value.

4.4.4. RBF Kernel Optimization OF Objective Functions

Kernels are commonly used to model non-linear data and play a key role in models like SVM. However, optimizing their parameters to best suit each dataset is a common challenge; poor selection of kernel parameters can lead to suboptimal model performance.

The kernel matrix is now included in the optimization problem, which is still the same (Wei et al., 2023):

$$Maximize \frac{1}{2} \sum_{i,j} \alpha_i \alpha_j y_i y_j K(x_i, x_j) - \sum_{i=1}^{N} \alpha_i \tag{8}$$

Subject to: $\alpha_i \geq 0$ and $\sum_{i=1}^{N} \alpha_i y_i = 0$

4.4.5. Decision Criterion

The classification decision rule is (Rahmani et al., 2024):

$$f(x) = sign(\sum_{i=1}^{N} \alpha_i y_i K(x_i, x_j) + b) \tag{9}$$

5. EXPERIMENTAL PROTOCOL

The Ten people who participated in this experiment, split into two separate groups. Five subjects make up the first group, which is referred to as the "lying" group, and five individuals make up the second group, which is referred to as the "innocent" group. The focal point of the experimental configuration is a visual stimulus that is displayed on a screen that is one meter away from the participants. This screen shows six pictures of different people from each session; each picture is shown for around two seconds, as illustrated in Fig. 10.

These images are categorized into three types:

- Probe (P) stimuli: These appear when a participant looks at a photo of a person they know only personally.
- Target (T) stimuli: These occur when the subject views a picture of a well-known public figure that members of both groups are all familiar with.
- Irrelevant (I) stimuli: These happen when a participant views an image of an unknown person chosen from a library of artificial intelligence profiles of unknown people.

Every three seconds, in between each stimulation, a blank image is shown. One session lasts for thirty seconds in total. Every participant undergoes three sessions, separated by rest periods to avoid headaches that could impede EEG data and introduce noise. As shown in Fig. 9, the timeline connected to the screen is captured. Based on this timeline, all EEG signals are captured and segmented based on the stimulus that was experienced.

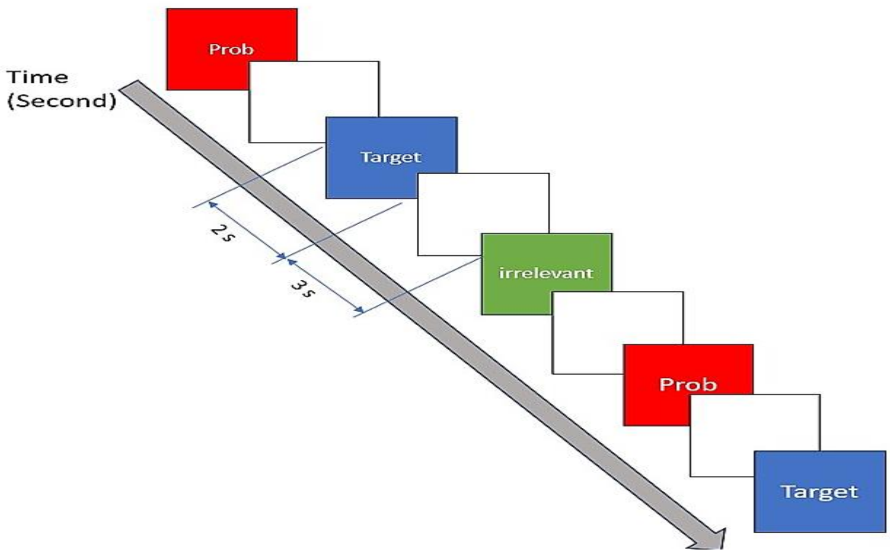

Fig. 9. Two feature distributions concerning output.

5.1. results

Following the execution of the experimental protocol with ten participants, the respective file for each participant, obtained from the EEG device in CSV format, underwent processing using Python version 3.9. Grouping participants into "lying" and "innocent" categories, each group comprised five individuals, with every participant contributing to 3 sessions. This resulted in a cumulative total of 15 datasets within each group and an aggregate of 30 datasets across all participants, as indicated in Table 1. In each session, three distinct stimulus types of probes, irrelevant, and target were presented twice, each lasting for two seconds on the screen. This was followed by a three-second interval of a blank screen in the display sequence, as depicted in Fig. 10.

Table 1. Datasets of the proposed experiment

Group	No. of participants	No. of sessions	No. of datasets
Lying	5	3	5 x 3 = 15
Truthful	5	3	5 x 3 = 15
	Total No. datasets		30

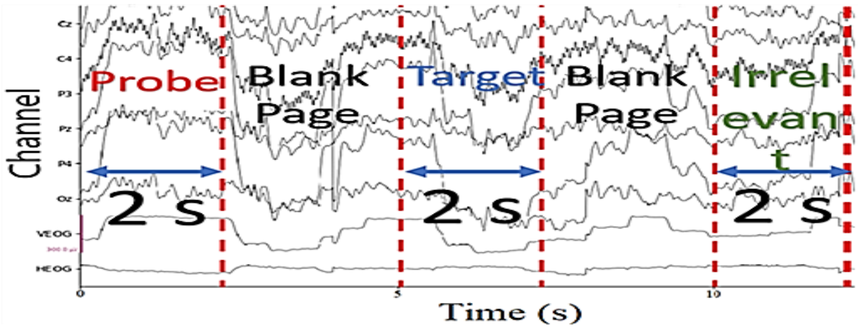

Fig. 10. The participant's EEG signal of one session.

5.2. Signal Processing Results

Within this section, the outcomes of EEG signal processing at each phase of this module will be showcased. The objective is to illustrate the successful mitigation of accompanying noise and to enhance the SNR. A comparison with other related studies will be conducted to highlight the significant contributions of this research.

5.3. ICA results

The principal aim of employing Independent Component Analysis is to mitigate ocular-related artifacts resulting from eye movements, blinking, and the interference of neighboring electrodes with each other. Fig. 10 showcases the effectiveness of this technique, where Fig. 11 (a) illustrates the sample EEG signal before applying ICA, and Fig. 11 (b) displays the sources of EEG signals after the utilization of ICA.

Following the elimination of all excluded components and the subsequent reverse transformation of the data, Fig. 12 displays the reconstructed EEG signal.

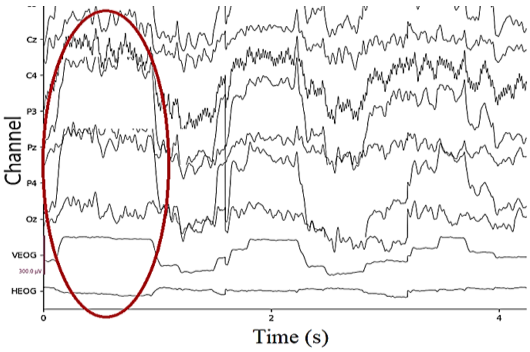

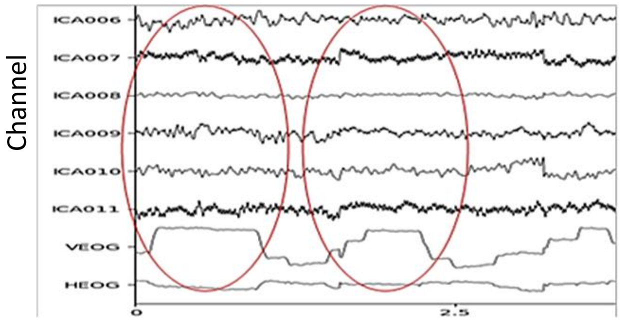

(a) **(b)**

Fig. 11. – (a) sample of raw EEG signal.; (b) sample of Independent Components (ICs).

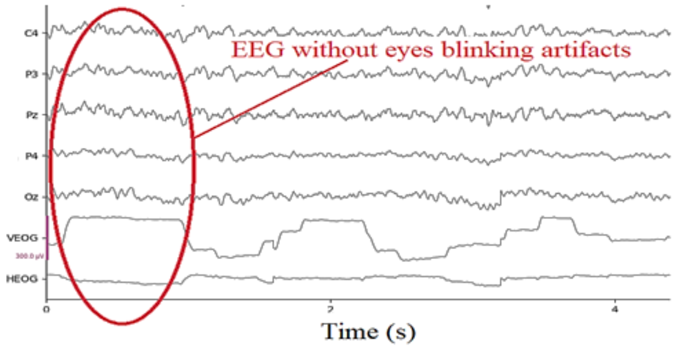

Fig. 12. Reconstructed EEG after applying ICA.

5.4. Epoch EEG Signals

Post executes the ICA, yielding EEG data devoid of eye movement or blinking effects, the EEG signal undergoes segmentation into epochs contingent on the type of stimulus, as shown in Fig.13 which illustrate the EEG signal and the epochs that need to be extracted.

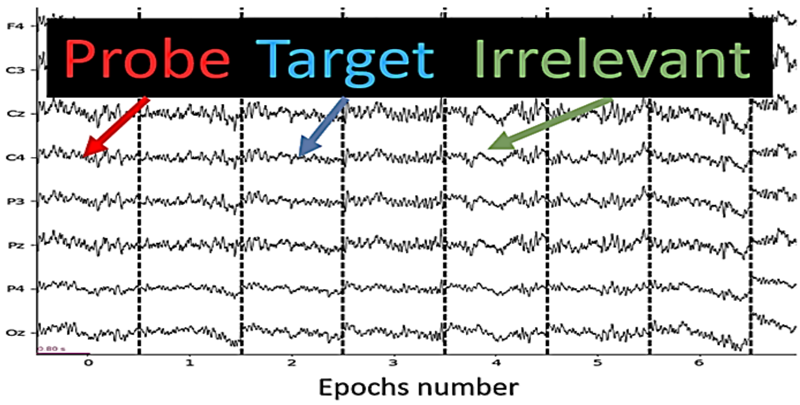

Fig. 13. Epochs of EEG signal after ICA.

5.5. ERP and P300 Result

Event-related potential is a signal that reflects the brain's response to a stimulus, as this effect may not manifest clearly within a single trial in the EEG signal. To capture this response more distinctly, ERP employs stimuli derived from a group of trials and computes their average. Illustrated in Fig. 14, the average signal was computed for probe (prob) stimuli (as depicted in

Fig. 14 (a, b)), target stimuli (as shown in Fig. 14 (c, d)), and irrelevant stimuli (as presented in Fig. 14 (e, f)) for both lying and innocent subjects. P300 signal is characterized by the amplitude at 300 milliseconds post-stimulus. This signal serves as a crucial indicator for determining whether an individual is lying or not.

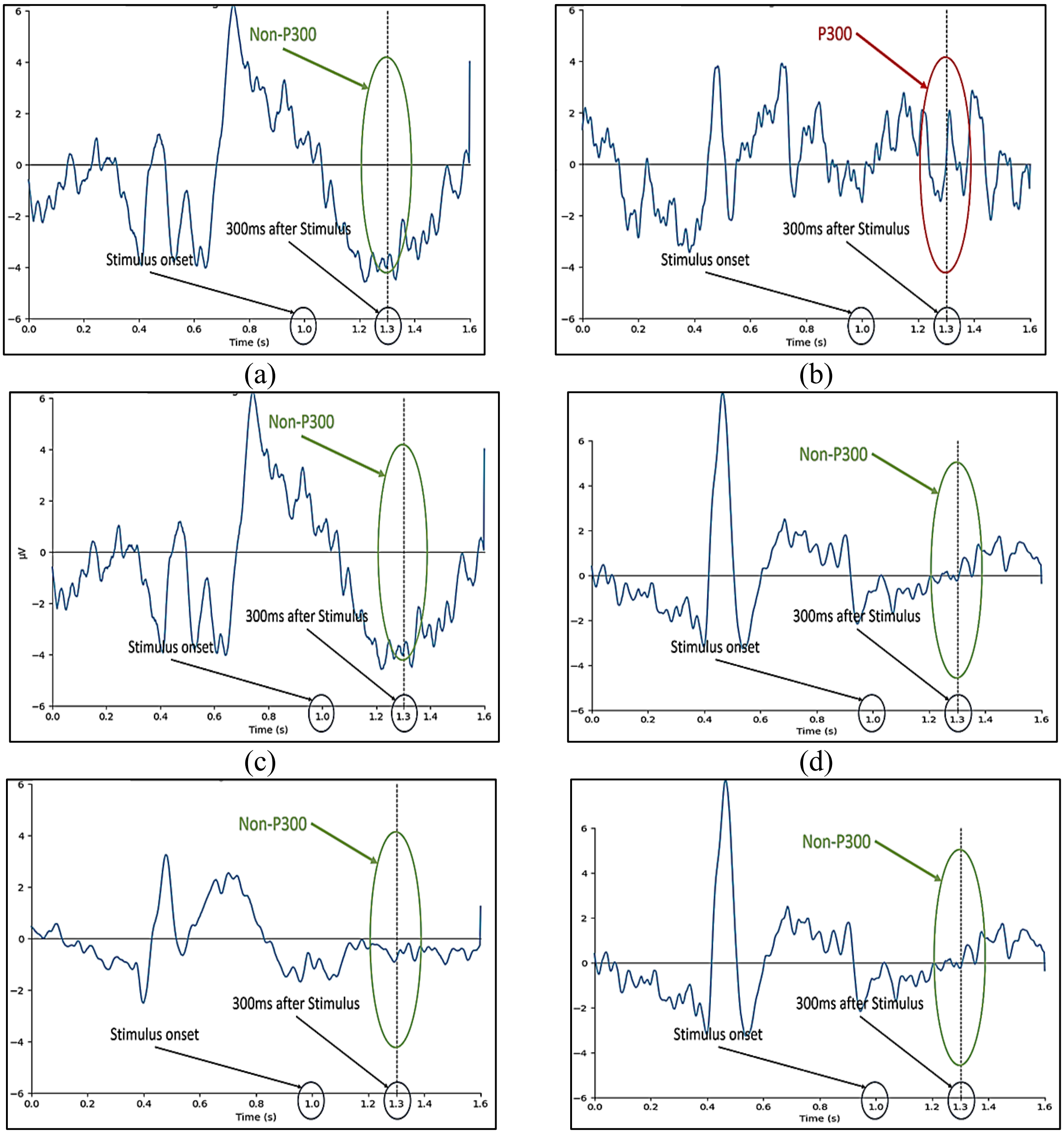

(a) (b) (c) (d) (e) (f)

Fig. 14. – P300 and non-p300 for (a) Probe stimuli (innocent); (b) Probe stimuli (lying); (c) Target stimuli (innocent); (d) Target stimuli (lying); (e) Irrelevant stimuli (innocent); (f) Irrelevant stimuli (lying)

5.6. Regression Baseline Correction

By employing this technique, the signal's drift within each epoch is eliminated, resulting in increased stability and freedom from slow, low-frequency variations present in the original data. Additionally, it ensures that the stimulus appears at the same time in each epoch. The effectiveness of this technique becomes apparent during the averaging process of epochs with similar stimuli, especially when contrasted with the traditional baseline correction method (blue color wave) that lacks the utilization of regression-based baseline correction (yellow color wave), as shown in Fig. 15 below.

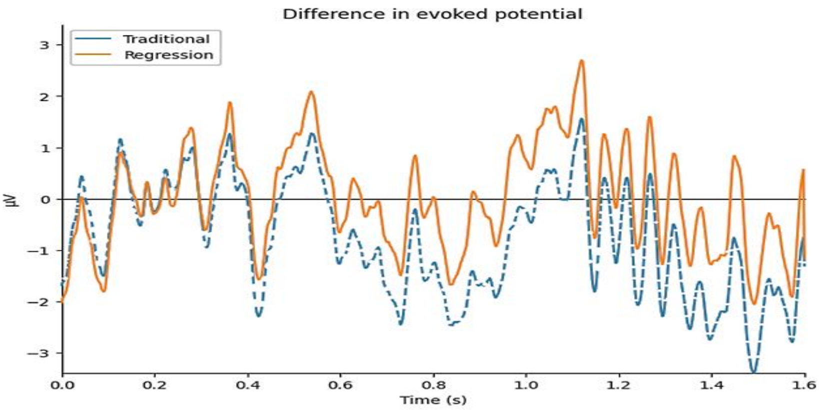

Fig. 15. The effect of regression-based baseline correction.

5.7. Classification Results

The training set constitutes a subset of information used to train a machine-learning model. It comprises instances (data points) where the desired outcome is already known. To enhance its accuracy in making classifications, the model adjusts its weights by identifying patterns and correlations within the training data. The data was split into two groups: one for lying and one for telling the truth. The lying data specifically includes information related to the Probe stimulus from the lying group, as shown in Fig. 15. This choice was made because it's the only situation where participants deny something, while all other stimuli represent honest and truthful responses. Another segment of the dataset, known as the test dataset, remains untouched during the model training process. Its sole purpose is to evaluate the trained model's effectiveness and its ability to generalize to new data. In this thesis, 40% of the dataset is allocated for testing the algorithms.

As illustrated in Tabel 2 to assess the performance of the three classification algorithms SVM, DBN, and LDA. An accuracy parameter was employed. The selection of this parameter is contingent on the characteristics of this work and the objectives of the analysis.

Table 2. All four parameters to evaluate the proposed classification algorithm

Parameters	Results
Accuracy	78%
Precision	0.9
Recall	0.92
F1 Score	0.45

The k-fold cross-validation technique was employed to enhance the reliability of the machine learning classification results. Additionally, 20% of the dataset was selected as training data. This process repeats k times (k=5), each time using a different fold as the test set and the remaining folds for training. The performance scores from each fold are averaged to get an overall estimate of the model's performance. As shown in the table below.

It is observed from the table that when the dataset size used is reduced from 40% to 20%, the accuracy decreases by nearly 1%.

Table 3. accuracy based on K-fold iteration

K-fold	Accuracy
Iteration 1	77.19586%
Iteration 2	77.19662%
Iteration 3	77.19675%
Iteration 4	77.19675%
Iteration 5	77.19675%
Mean	77.196546

5.8. Comparison Results with Other Studies

In 2020, Divyanshu Singh (Baghel et al., 2020) conducted a study on automated lie detection from EEG signals using a convolutional neural network (CNN) and a deep learning approach. The author's model processes 14-channel EEG data to discern between truthful and deceptive assertions. The CNN structure, with varying numbers of neurons and activation functions like a sigmoid, hyperbolic tangent, and rectified linear unit (ReLU), was evaluated for truth identification, achieving an accuracy of up to 84.44%. The proposed method applied the same dataset as outlined in Table 4, resulting in an increased accuracy of 86% for distinguishing between falsehood and truth. This represents a 2% enhancement in accuracy compared to the referenced study.

Table 5 illustrates the classification accuracy comparison when using the data utilized by (Baghel et al., 2020) in this study module.

Table 4. Dryad datasets were used in the experiment (Baghel et al., 2020)

Category	Sub-category	Total samples
Innocent	Innocent irrelevant	50
	Innocent probe	50
	Innocent target	50
Lying	Lying irrelevant	50
	Lying probe	50
	Lying target	50
Total	300	

Table 5. Total datasets and classification accuracy

Datasets	No. Of datasets	accuracy
Proposed method	300	86%
(Baghel et al., 2020)	300	84.44%

6. CONCLUSIONS

This research suggests a framework aimed at improving the identification of falsehood by utilizing EEG signals. The signals are recorded using an EEG device, and then a signal processing module employs diverse methods to acquire P300-ERP signals. Afterward, feature extraction is executed, and machine learning algorithms for categorization are suggested. This research results in the subsequent findings:

1. When using the same dataset employed in (Baghel et al., 2020), an increase of nearly 2% in classification accuracy was achieved. This improvement can be attributed to the signal denoising process utilizing the signal processing model in Flowchart 1.

2. Due to the SVM algorithm's ability to consolidate categorized features within the same class and establish a clear separation from features in the opposite class, preventing point blending, the highest classification accuracy of 78% was achieved with the SVM algorithm. This was determined through data collected from 10 participants, as described in the experimental protocol (Section 4). Three types of algorithms were tested: SVM, DBN, and LDA.

In the future, we will increase the dataset size by expanding the number of participants in the experiment to achieve the highest possible classification accuracy. in addition, we can interlace signals from other sources, such as ECG signals, in addition to incorporating facial and eye gesture monitoring using cameras.

7. REFERENCES

Ali, S.M. and Hameed, H.A. (2020) 'Hand image verification method based on PCA eigenvectors', Journal of Kufa-Physics, 3(1).

Bablani, A., Edla, D., Kuppili, V. and Dharavath, R. (2021) 'Lie detection using fuzzy ensemble approach with novel defuzzification method for classification of EEG signals', IEEE Transactions on Instrumentation and Measurement, 70, 1–13.

Bablani, A., Edla, D.R., Kuppili, V. and Ramesh, D. (2020) 'A multistage EEG data classification using k-means and feed forward neural network', Clinical Epidemiology and Global Health, 8, 718–724.

Baghel, N., Singh, D., Dutta, M.K. et al. (2020) 'Truth identification from EEG signal by using convolution neural network: Lie detection', IEEE 43rd International Conference on Telecommunications and Signal Processing (TSP), 550–553.

Chao, H. and Liu, Y. (2020) 'Emotion recognition from multi-channel EEG signals by exploiting the deep belief-conditional random field framework', IEEE Access, 8, 33002–33012.

Gao, J., Gu, L., Min, X. et al. (2022) 'Brain fingerprinting and lie detection: A study of dynamic functional connectivity patterns of deception using EEG phase synchrony analysis', IEEE Journal of Biomedical and Health Informatics, 26(2), 600–613.

Gao, J., Min, X., Si, H. et al. (2022) 'Effective connectivity in cortical networks during deception: A lie detection study based on EEG', IEEE Journal of Biomedical and Health Informatics, 26(8), 3755–3766.

Gu, L., Jiang, J., Han, H. et al. (2023) 'Recognition of unilateral lower limb movement based on EEG signals with ERP-PCA analysis', Neuroscience Letters, 800.

Kappenman, E., Farrens, J., Zhang, W. et al. (2021) 'ERP CORE: An open resource for human event-related potential research', NeuroImage, 225.

Kokate, P., Pancholi, S. and Joshi, A. (2021) 'Classification of upper arm movements from EEG signals using machine learning with ICA analysis', arXiv preprint.

Lin, X., Sai, L. and Yuan, Z. (2018) 'Detecting concealed information with fused electroencephalography and functional near-infrared spectroscopy', Neuroscience, 386, 284–294.

Obais, Z. and Hasan, T. (2020) 'Classification of non-invasive recording of electroencephalography brain signals using Hoeffding tree', Journal of Kufa for Mathematics and Computer, 7(1).

Pooja, S., Pahuja, S. and Veer, K. (2022) 'Recent approaches on classification and feature extraction of EEG signal: A review', Robotica, 40(1), 77–101.

Rad, D., Paraschiv, N. and Kiss, C. (2023) 'Neural network applications in polygraph scoring—A scoping review', Information, 14(10).

Rahmani, M., Mohajelin, F., Khaleghi, N., Sheykhivand, S. and Danishvar, S. (2024) 'An automatic lie detection model using EEG signals based on the combination of type 2 fuzzy sets and deep graph convolutional networks', Sensors, 24(11).

Supriya, S., Siuly, S., Wang, H. et al. (2023) 'Epilepsy detection from EEG using complex network techniques: A review', IEEE Reviews in Biomedical Engineering, 16, 292–306.

Wei, S., Gao, J., Yang, Y. et al. (2023) 'Analysis of weight-directed functional brain networks in the deception state based on EEG signal', IEEE Journal of Biomedical and Health Informatics, 27(10), 4736–4747.

Xiong, Y., Gu, L. and Gao, J. (2020) 'Phase synchrony and its application to lie detection', IEEE International Conference on Power, Intelligent Computing and Systems (ICPICS), 726–729.

Yue, Y., Plested, J. and Gedeon, T. (2020) 'Information-preserving feature filter for short-term EEG signals', Neurocomputing, 408, 91–99.

Zhou, J., Zhang, X. and Jiang, Z. (2021) 'Recognition of imbalanced epileptic EEG signals by a graph-based extreme learning machine', Wireless Communications and Mobile Computing.